

Modeling Microfluidic Separations using Comsol Multiphysics

Bruce A. Finlayson^{*1}, R. Anthony Shaw²

¹University of Washington, ²Institute for Biodiagnostics, National Research Council of Canada

*Corresponding author: Dept. Chem. Engr., Box 351750, Univ. Washington, Seattle, 98195-1750,
finlaysa@u.washington.edu

Abstract: Infrared spectroscopy can be used to identify and quantify individual (bio)chemical species within complex mixtures provided the spectroscopic fingerprints are strong enough. It is often the case, however, that the characteristic fingerprints are concealed by the much stronger absorptions of the most concentrated species. For example, in the case of blood serum, the very strong absorptions of protein severely hinder detection of diagnostically relevant metabolites. A microfluidic device [1,2] is modeled here with the objective of separating serum metabolites from proteins, or – more precisely – to enhance the metabolite/protein concentration ratio, and in so doing to provide a new metabolite-rich sample for spectroscopic characterization [3-5]. Focusing upon a representative metabolite (creatinine) and protein (albumin) we have modeled the diffusion of serum components into a water stream when the two streams flow in contact through a microchannel. With the laminar fluid diffusion interface (LFDI) thus created, creatinine diffuses rapidly into the water, while the albumin hardly diffuses at all. Thus, at the channel exit one may recover a product containing significant creatinine but very little albumin.

The goal of the simulations is to predict the composition of the product stream. To that end, we have tested various two-dimensional models to see if the essential features are contained in them. Various fluid mechanical insights are found: diverging flow at the inlet, converging and separating flow at the exit, and the difference between 2D and 3D simulation results.

Keywords: microfluidics, flow, diffusion

1. Introduction

While the LFDI channel is incorporated within a larger laminated microfluidic card that includes reservoirs, valves, etc. to direct the flow of serum and water into the channel (and recover the product from it), this investigation focuses only on flow and diffusion within the LFDI channel. The geometry of the channel is shown in Figures 1 (vertical view) and 2 (two-dimensional side view). Simulations of flow and convective diffusion are done in and three dimensions to determine the effect of the viscosity ratio, inlet and exit geometry, and to establish a simple design procedure to predict the concentrations in the product stream.

The rectangular section of the LFDI channel is 22 mm long, 4.5 mm wide and 330 mm high. The cone shape at the inlet (and outlet) is 4 mm long. The sample and receiver streams are separated by a 127-micron divider that extends into the cone-shaped channel entrance – the “priming area”. In contrast, the channel converges at the exit while the streams are still in contact – the 127-micron divider is at the very end of the tapered LFDI channel.

For the purpose of developing and validating the simulation methodology, we specify receiver and sample flow rates of 1.84 $\mu\text{L/sec}$ and 1.02 $\mu\text{L/sec}$, respectively. The viscosity of the water is 1 mPa s, and the water density is 1 g/cm³. The viscosity of the serum entering is assumed to be 1.57 mPa s (serum viscosity is variable – this is marginally higher than the average), and the

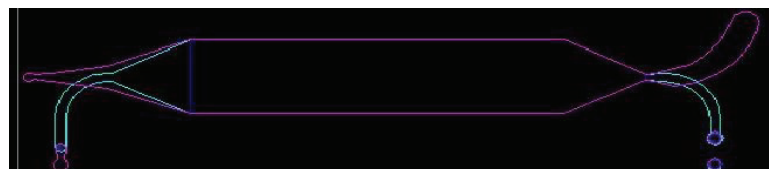


Figure 1. Laminar fluid diffusion interface (LFDI) channel
(Top view, illustration courtesy of Micronics, Inc., Redmond, WA)

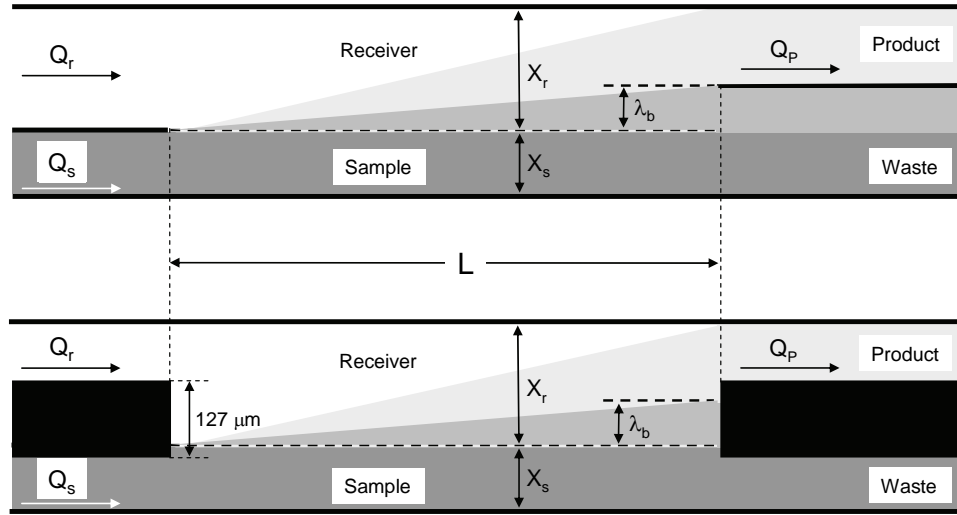


Figure 2. Schematic of the separation of creatinine (light grey) and albumin (dark grey) (a) with knife edge; (b) with blunt ends

serum density is taken as 1 g/cm³. The diffusivities of creatinine and albumin in both the serum and water streams are 9.19×10^{-10} m²/s and 6.7×10^{-11} m²/s, respectively. The Reynolds number in the rectangular part of the channel is 0.634, based on the height of the channel, the average velocity, and the density and viscosity of water. The Peclet numbers are 689 (creatinine) and 9460 (albumin), based on the average velocity, height of the channel, and diffusivity in water.

2. Analytical solution when fluids are immiscible

Since the serum and receiver fluid streams scarcely mix (see below), insight can be obtained by looking at Poiseuille flow of two immiscible fluids between flat plates. Because the flow profile is essentially quadratic, the height of the sample (serum) stream is not simply proportional to the flow rate ratio Q_s/Q_{tot} (Q_{tot} is the total flow rate, i.e. the sum of sample plus receiver flow rate $Q_s + Q_r$). Fully developed flow of two immiscible fluids between two flat plates is solved in Bird, *et al.* [6], when the two fluids take up exactly the same space (i.e. the thickness of each fluid is one-half the total thickness). That solution is generalized here to allow any fraction, which ultimately will depend upon the flow rate

ratio. The notation follows that of Bird, *et al.* and the derivation and discussion are elsewhere [7].

Figure 3 shows the geometry. The flow rates of the two fluids are

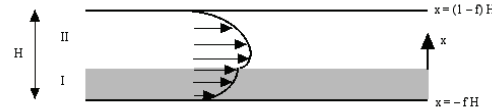


Figure 3. Flow of two immiscible fluids between parallel plates

$$\begin{aligned} Q_1 &= -\frac{\Delta p}{6\mu_1 L} (fH)^3 + \frac{C_1}{2\mu_1} (fH)^2 + C_2 (fH) \\ Q_2 &= -\frac{\Delta p H^3}{6\mu_2 L} (1-f)^3 - \frac{C_1 H^2}{2\mu_2} (1-f)^2 + C_2 H (1-f) \\ C_1 &= \frac{\Delta p H \mu_2 f^2 - \mu_1 (1-f)^2}{2L} \frac{\mu_2 + (1-f)\mu_1}{f\mu_2 + (1-f)\mu_1}, \\ C_2 &= \frac{\Delta p H^2}{2L} \frac{f(1-f)}{f\mu_2 + (1-f)\mu_1} \end{aligned}$$

where μ_1 and μ_2 are the viscosities of serum and water respectively, H the channel height (330 μm), Δp the channel entrance/exit pressure differential, and f the fractional channel height occupied by the serum stream. If a specific f is sought, one can solve for the flow rates. If the flow rates are specified, though, one must solve

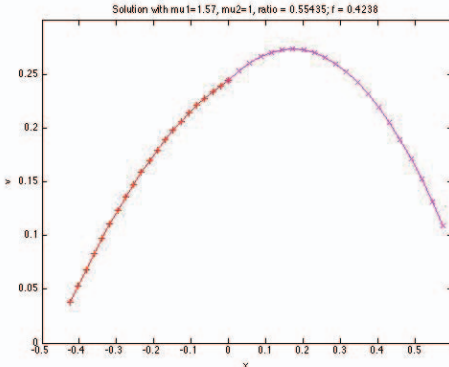


Figure 4. Velocity profile for two immiscible fluids flow between flat plates when $R = Q_1/Q_2 = 0.554$.

for the value of f that gives the correct ratio of flow rates, Q_1/Q_2 .

When the two viscosities are equal and $f = 0.5$, this should give the equation for a fully developed flow between two parallel plates, which it does. When $R = Q_1/Q_2 = 0.554$ (i.e. for the flow rates of interest here; $Q_r = 1.84 \mu\text{L/sec}$ and $Q_s = 1.02 \mu\text{L/sec}$), for $\mu_1/\mu_2 = 1.57$, the $f = 0.424$. The velocity profile is shown in Figure 4. If the same program is run with $R = 1$, and equal viscosities, a parabolic profile is obtained, as expected.

3. Use of COMSOL Multiphysics

Comsol Multiphysics is used to solve the three-dimensional flow of a Newtonian fluid in this geometry, followed by the solution of the convective diffusion equation for each chemical. Comparisons are made with two-dimensional simulations to see whether the two-dimensional simulations capture the essential features, qualitatively and quantitatively. For this study, the viscosity is taken as the same in both fluids, 1 mPa s . For applications the key results are the fractional recovery of each chemical (creatinine and albumin) going out the product stream (the fraction of the stream above the “diffusion barrier” λ_b , of Figure 2) and the enhancement in the concentration ratio of creatinine/albumin.

$$\text{enhancement ratio} = \frac{\int c_{\text{creatinine}} u dA}{\int c_{\text{albumin}} u dA}$$

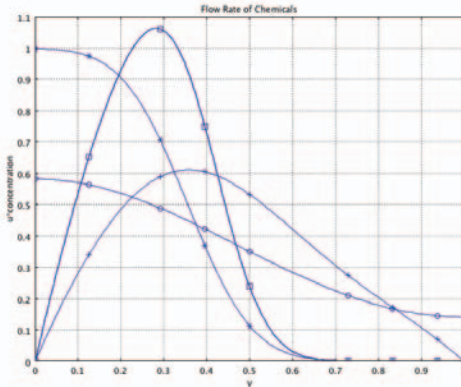


Figure 5. Comparison of outlet concentration*velocity for creatinine (lower curves) and albumin (upper curves) when the velocity is constant ($\circ, *$) and quadratic ($+, \square$).

3.1. Diffusion model

The simplest model would be a two-dimensional one with plug flow (constant velocity across the channel height). However, that leads to incorrect results, as seen below. The next simplest model is to solve the problem with a quadratic velocity profile, which is appropriate when the viscosities of the two fluids are the same: $u = 6y(1-y)$. Now the dimensionless diffusion problem is

$$6y(1-y) \frac{\partial c}{\partial x} = \frac{1}{Pe} \frac{\partial^2 c}{\partial y^2}$$

The initial conditions must be changed slightly to ensure that the same amount of material enters, since the velocity is small near each wall. This problem is solved using the analytical solution for two immiscible fluids (viscosity ratio of 1.0) and the same flow rate ratio = 0.55435. The fractional channel height occupied by the serum stream is $f = 0.4032$. Thus, the initial/boundary conditions are

$$c(y,0) = 1, y \leq 0.4032, 0 \text{ otherwise}; \quad \frac{\partial c}{\partial y} = 0 \text{ at } y = 0, 1$$

This problem is solved in Comsol Multiphysics with the following initial condition.

$$ystep = flc1hs(0.4032-y, 0.01)$$

The problem is integrated until $x = 66.7$. The product of velocity and concentration (flux) is shown in Figure 5, which also shows the corresponding solutions for a constant velocity profile ($u = 1$). As can be seen there, because of the parabolic profile, the fractional recovery of albumin (and, to a lesser extent, creatinine)

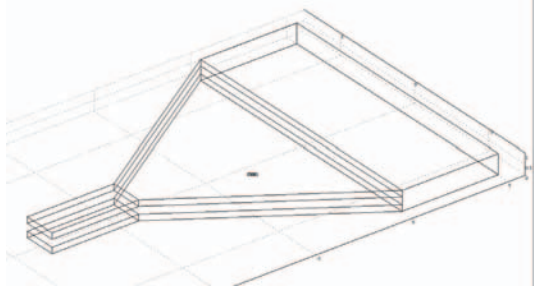


Figure 6. Three-dimensional inlet

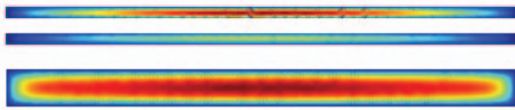


Figure 7. Velocity at end of expansion (a) and outlet (b) of 3D inlet

depends strongly on where the product/waste cutoff is placed, i.e. on the height of the diffusion barrier (λ_b of Figure 2). For example, if only the fraction of the stream that emerged above $y = 0.7$ is aspirated as product, very little albumin is collected.

3.2. Inlet region

The geometry at the inlet is shown in Figure 6 (see also Figure 2b, which highlights the 5-mil (127-micron) divider that separates the sample and receiver streams until they converge at the beginning of the LFDI channel proper). We focus now on the question of how the streams behave and interact as they flow around the divider and begin the journey along the LFDI channel. For clarity, Figure 6 truncates the device at five channel-heights downstream in order to concentrate on the effect of the expansion of the two layers into the rectangular parallelepiped. The flow was solved with 186,531 elements (906,794 dof), and the convective diffusion equation was solved with 564,316 elements (841,579 dof).

The flow at the end of the expansion and the outlet are shown in Figure 7. Whereas there is a significant difference in velocity at the end of the expansion (since the flow rates are different), by the time the fluid reaches the end (five channel-heights downstream) the flow profile is simply that of flow in a tube with a rectangular cross section.



Figure 8. Concentration out of narrow neck; (a) creatinine, (b) albumin

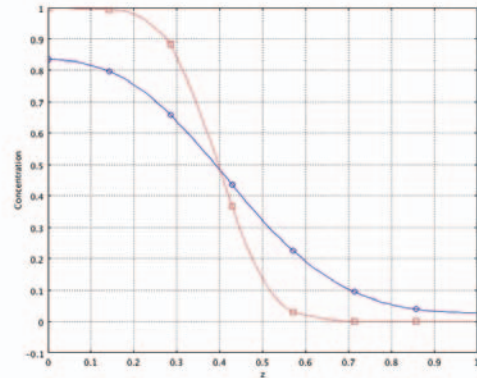


Figure 9. Concentration of creatinine (circle, blue) and albumin (square, red) at exit

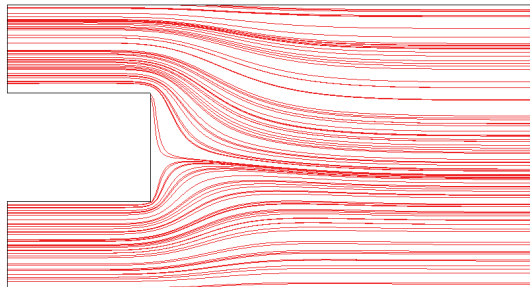


Figure 10. Streamlines at inlet in 2D model

Similarly, the concentration profiles of creatinine and albumin at the end of the expansion are a constant dimensionless concentration of 1. At the exit of the geometry shown in Figure 6 the creatinine and albumin profiles are similar over most of the width, with expected changes near the side boundaries (Figure 8). At the exit corner the concentration profiles are shown in Figure 9 (when one-half the domain was solved). There are not enough elements at the end to obtain a sharp profile for albumin. However (see below), the variances are similar in the 2D and 3D models.

For these conditions the average concentration is always 0.3566, and variances is defined as:

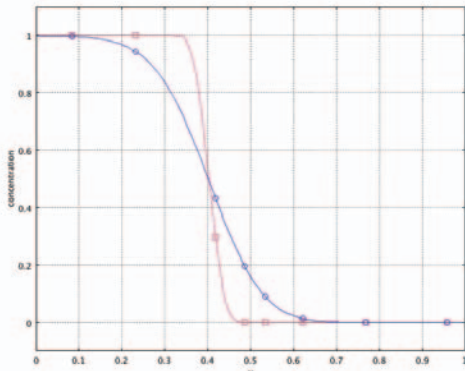


Figure 11. Concentration of creatinine (circle, blue) and albumin (square, red) at exit

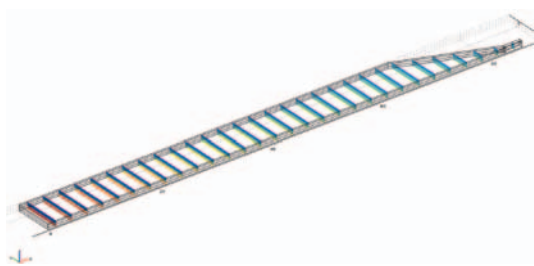


Figure 12. Concentration of creatinine in exit geometry

$$c_{\text{var}} = \frac{\int (c - c_{\text{avg}})^2 u dy}{\int u dy}.$$

The streamlines for a 2D model are shown in Figure 10, which shows the stagnation flow of the two streams towards each other at the blunt end, and the lowered dividing streamline reflecting the relatively high receiver fluid flow rate ($Q_r=1.84 \mu\text{l/sec}$) as compared to that of the sample ($Q_s=1.02 \mu\text{l/sec}$). The concentration profiles at the exit are shown in Figure 11. Here 25,181 degrees of freedom were used. The variances of creatinine are 14% in 3D, 15% in 2D; for albumin they are 20% in 3D, 21% in 2D. These results indicate that a two-dimensional model of the inlet suffices, but that some diffusion occurs in a distance downstream equal to five times the height.

3.3. Exit Region

The exit region is modeled as shown in Figure 12. The exit geometry modeled here contains a knife-edge (the idealized situation of Fig. 2a) contained between $x = 0.641$ and 0.643 rather than a blunt end (Fig. 2b).

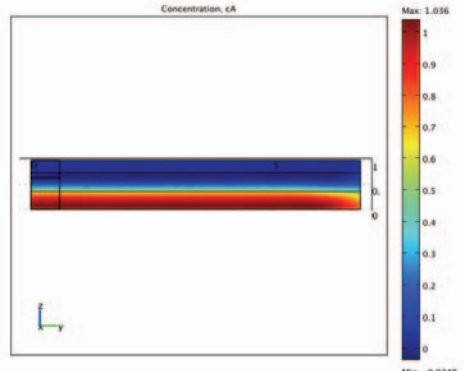


Figure 13. Concentration of albumin at a distance of 65 where channel starts to narrow

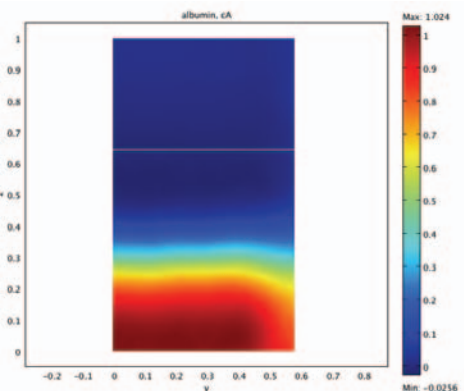


Figure 14. Concentration of albumin at exit

The inlet boundary condition was the fully developed velocity in a rectangle; the outlet boundary condition was laminar outflow. A total of 376,934 degrees of freedom were used to model the flow, and the mass balance at any distance downstream was correct to 0.17%. For the purpose of this simulation, the fraction of flow out the top is 18.5% and is set by the outlet boundary condition. In practical use of the LFDI technique, the fraction of flow collected as product (“out the top”) is dictated by the aspiration flow rate for a pump that actively aspirates the product from the LFDI channel outlet, i.e. the diffusion barrier height is dictated by the aspiration flow rate.

The concentration of creatinine was solved using 287,446 degrees of freedom. The inlet concentration was taken as 1.0 in the bottom section and 0.0 in the top section; the sample/receiver interface height was determined by solved for f when the flow rates are given and the viscosity is the same everywhere (this is only an approximation to the output from the inlet

section just discussed, but it is close). The mass balances for creatinine were within 0.2% of each other. When albumin was considered, more elements were necessary because of the high Peclet number; 570,849 degrees of freedom were used, giving a mass balance accurate within 0.3%.

The concentration of albumin at the point where the channel narrows is shown in Figure 13 and at the exit in Figure 14. While 18.5% of the flow goes out the top, only 13% of the creatinine goes out the top. For albumin only 0.28% goes out the top, showing the effect of relatively fast creatinine diffusion.

For the two-dimensional model, the velocity is a quadratic function of position, zero at both top and bottom boundary, while the concentration is taken as 1 in the lower section and 0 in the upper section. While the 2D model can't account for the effect of the distal narrowing of the LFDI channel, what matters is what fraction of the creatinine and albumin go out the top. The results are 14% and 0.055% for creatinine and albumin, respectively, compared with 13% and 0.28% in the 3D model. Thus, the 2D model suffices for the creatinine but not for the albumin.

The effect of a knife-edge versus a blunt end at the exit depends, of course, on the flow rates studied. For the case where 35% of the flow goes out the top (product aspiration rate $Q_p = 1.02 \mu\text{l/sec}$), the diffusion barrier is lower and more creatinine and albumin are recovered. The results for creatinine were very similar to one another, i.e. 23.5-23.6% out the top in both cases. For albumin, however, the knife-edge exit resulted in 0.23% whereas the blunt exit gave 0.36%.

A similar study at the entrance comparing a knife-edge with a blunt edge resulted in almost identical results at a distance downstream of five times the height. Thus, the concentration profile is not strongly dependent on the shape of the inlet.

4. Effect of Viscosity Ratio

A two-dimensional exit problem is solved with a blunt end and with a viscosity that depends upon concentration.

$$\eta = 1 + 0.57 * cA$$

This is an approximation for the effect of albumin on the viscosity. However, since the albumin hardly diffuses, the viscosity of the

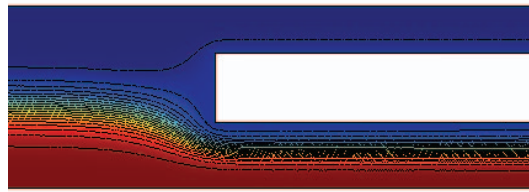


Figure 15. Relative viscosity near the outlet; blue = 1, red = 1.57.

product (bottom exit) remains very near the nominal serum viscosity of 1.57 (dimensionless). The flow and concentrations were solved using 104,262 elements and 476,678 degrees of freedom for flow and 211,523 degrees of freedom for each concentration. Thus, almost one million degrees of freedom were solved for. Because of the viscosity difference, the dividing streamline for the inlet is at 0.4238, corresponding to a ratio of flow rates of 0.55435 and a viscosity ratio of 1.57. The flow out the top is 0.357 of the total flow, which places the top of the diffusion barrier a distance $f = 0.4032$ from the *top* of the LFDI channel.

Figure 15 illustrates the viscosity gradient at the LFDI channel outlet. Note that the receiver fluid (metabolite-enriched water, with minor protein contamination) goes out the top and bottom, whereas the sample fluid (serum, with albumin concentration near the original value) mainly goes out the bottom; the concentration profile of albumin looks almost identical to Figure 15. The fraction of creatinine in the product (i.e. the fluid that exits above the diffusion barrier) is 24%, while that of albumin is 0.58%. This gives an enhancement factor of 41. The figures are very similar to what would be obtained with a viscosity ratio of one, except that then the fraction of albumin out the top is 0.36%, giving an enhancement factor of 66. Thus, the effect of a variable viscosity is to lower the enhancement factor, at least in this case.

5. Design Procedure

Based on these results, the following design procedure can be employed. **Step One:** For a fixed ratio of inlet flow rates, find where the dividing streamline will be, using the results for an immiscible fluid. Here that value was at 0.4032 when i) the velocity profile was quadratic, ii) the flow rate of the lower stream

was 0.554 times the flow rate of the upper stream, and iii) the viscosities were equal for the sample and receiver streams. After the perturbation due to the inlet disappears (it essentially does by 5 channel-heights downstream), the dividing streamline forming the sample/receiver interface lies at a height where the concentration would be 1.0 below the streamline and 0 above it, if there were no diffusion. **Step Two:** Then use an approximate solution [8] to estimate the width of the diffusion layer at a certain channel length. Here the length is $x = 66.7$, and the diffusion layer thickness is given, approximately, by

$$\delta(t) = \sqrt{12t} = \sqrt{12x/Pe}$$

Since the Peclet number is defined in terms of the average velocity, and the velocity at the dividing streamline is different, this formula can be revised as follows. The average velocity is 1.0, the peak velocity is 1.5, and the velocity at the dividing streamline is $1.5*[1-(0.5-0.4032)/0.5]^2 = 1.44$ times the average velocity

$$\delta(t) = \sqrt{12x/1.44 * Pe}$$

For a length of 66.7 and a Peclet number of 689 (creatinine), that thickness is 0.90, which indicates that the creatinine diffusion layer has reached the upper surface. For a length of 66.7 and a Peclet number of 9460 (albumin), that thickness is 0.24. Thus, adjusting the flow rates so as to place the diffusion barrier at a fractional height of $0.40+0.24 = 0.64$ would, to this approximation, cause nearly all the albumin to go out the bottom. This estimate can then be refined using Comsol Multiphysics to solve the complete problem.

6. Conclusions

The device can be modeled reasonably well with a two dimensional model. The shape of the inlet (blunt or knife-edge) makes little difference, but the product composition is affected by the blunt divider (as opposed to knife-edge) at the channel exit. Large enhancements in the metabolite/protein ratio can be obtained, opening the door to sensitive metabolic fingerprinting measurements using infrared spectroscopy.

7. References

1. Brody, J. P.; Yager, P., Diffusion-based extraction in a microfabricated device, *Sens. Actuators A Phys.* **58**, 13–18 (1997).
2. Jandik P.; Weigl B. H.; Kessler, N.; Cheng, J.; Morris, C. J.; Schulte, T.; Avdalovic, N., Initial study of using a laminar fluid diffusion interface for sample preparation in high-performance liquid chromatography, *J Chromatogr. A.* **954**, 33–40 (2002).
3. Mansfield, C. D.; Man, A.; Low-Ying, S.; Shaw R. A., Laminar fluid diffusion interface preconditioning of serum and urine for reagent-free infrared clinical analysis and diagnostics, *Appl. Spectrosc.* **59**, 10-15 (2005).
4. Mansfield, C. D.; Man, A.; Shaw, R. A., Integration of microfluidics with biomedical infrared spectroscopy for analytical and diagnostic metabolic profiling, *IEE Proc. Nanobiotech.* **153**, 74-80 (2006).
5. Shaw, R. A.; Rigatto, C.; Reslerova, M.; Low Ying, S; Man, A.; Schattka, B.; Battrell, C. F.; Matthewson, J.; Mansfield C., Toward point-of-care diagnostic metabolic fingerprinting: quantification of plasma creatinine by infrared spectroscopy of microfluidic-preprocessed samples, *Analyst*. **134**, 1224-1231 (2009).
6. Bird, R. B., W. E. Stewart, E. N. Lightfoot, "Transport Phenomena," 2nd ed., Wiley (2002), p. 56-58.
7. Finlayson, B. A., "Poiseuille Flow of Two Immiscible Fluids Between Flat Plates," to be submitted, 2010.
8. Finlayson, B. A., "The Method of Weighted Residuals and Variational Principles," Academic Press (1972), p. 45.

8. Acknowledgements

RAS thanks the Genomics and Health Initiative (National Research Council of Canada) and Canadian Institutes of Health Research for funding the ongoing integration of microfluidics with IR spectroscopy.